J Solid State Electrochem (2012) 16:165–171
DOI 10.1007/s10008-010-1287-2

ORIGINAL PAPER

Photoelectrochemical and optical characterization of Prussian blue onto p-Si(100)

Eduardo C. Muñoz · Rodrigo G. Henríquez · Ricardo A. Córdova · Ricardo S. Schrebler · Regina Cisternas · Luis Ballesteros · Ricardo E. Marotti · Enrique A. Dalchiele

Received: 10 November 2010 / Revised: 21 December 2010 / Accepted: 23 December 2010 / Published online: 26 January 2011

Abstract In this study, we examined the characterization of Prussian blue deposited onto p-Si(100). A cyclic voltammetry analysis was carried out under illumination showing quasi-reversibility responses of high and low-spin iron centres in the deposit. Optical measurements were done, where XRD analysis allowed to determine crystallinity while EDS analysis indicated that there is influence in the number of cycles on the film composition. Reflectance measurements confirm the coloration observed in the films. However a Kubelka–Munk analysis demonstrates the presence of blue greenish coloration which is an indication of a mix between Prussian blue and Berlin green films. Finally, this research is oriented to construct electrochemical storage devices which can be in situ loaded by the photovoltaic action of the semiconductor base material-doped silicon.

Keywords Prussian blue · P-silicon · Optical behaviour · Electrochemical behaviour

Introduction

The energy conversion has been the most important scientific and technological challenge during the last decades. In this context, the direct conversion of sun radiation into electricity is not only important but also the conversion and storage of this energy. One possibility is the use of semiconductors, which can take the energy photon and converts it into electrochemical energy. With this, it would be possible to transfer this electrochemical energy to solid layers deposited onto the semiconductor substrates and which are optical transparent to the photons that can reach the semiconductor. So, the solid compounds should be redox centres which could be oxidizing or reducing by means of the photons coming from the sun. In this context, silicon could be an interesting semiconductor considering its wide absorption in the electromagnetic spectra. On the other hand, the use of metallic hexacyanometallates on silicon electrodes (cathode and anode) with large separation in their formal potentials could accept electrons and/or holes producing a reduction or oxidation process in the metal centres which store the energy under electrochemical form. However, the principal problems are: optical transparency needs thin layers but this means short storage capacity, high chemical/electrochemical reversibility, among others.

For this reason, the aim of this work is to characterize Prussian blue deposited onto silicon p-type by means of electrochemical and optical techniques.

E. C. Muñoz (✉) · R. G. Henríquez · R. A. Córdova · R. S. Schrebler · R. Cisternas · L. Ballesteros
Instituto de Química, Facultad de Ciencias,
Pontificia Universidad Católica de Valparaíso,
Casilla,
4059, Valparaíso, Chile
e-mail: eduardo.munoz.c@ucv.cl

R. E. Marotti · E. A. Dalchiele
Instituto de Física, Facultad de Ingeniería,
Universidad de La República,
Herrera y Reissig 565, C.C. 30, 11000, Montevideo, Uruguay

Experimental section

Prussian blue deposition (PB) was performed on monocrystalline p-Si(100) with a resistivity between 0.01 and 0.3 Ω cm ($N_A \cong 5 \times 10^{17}$ cm^{-3}), B-doped and polished/etched surfaces (Int. Wafer Service, CA, USA). The silicon wafer was cut into rectangles (1.0 × 2.5 cm^2), and they were treated considering procedures used previously [1–5]. The

silicon area exposed to the solution was 1.0 cm^2. Before the experiments, the electrode surface was again etched for 2 min in 4% HF solution. For each measurement, a new electrode of p-Si(100) was used, due to the well-known fact that some metals can diffuse into the inner of silicon [6, 7].

For the voltammetric studies, a platinum wire was used as a counter electrode and mercury/mercury sulfate electrode (Hg/Hg_2SO_4, K_2SO_4 (saturated), 0.640 V vs. NHE) was used as a reference electrode. All the potentials reported in this study refer to this reference electrode.

The electrolytic solutions were prepared using distilled and deionized water (Millipore) with a resistivity of 18 MΩ cm. Analytical grade reagents from Merck (H_3BO_3, Na_2SO_4, K_2SO_4, Fe_2SO_4 $7H_2O$ and H_2SO_4) and Fluka ($K_4[Fe(CN)_6]\times 3H_2O$) were used.

The synthesis of the PB film for photoelectrochemical characterization was carried out with the following protocol: following the cleaning procedure (see above), the p-Si (100) electrode was mounted in the Teflon holder leaving 1 cm^2 as the electrode surface area exposed to the solution. Then the electrode was transferred to a cell containing 0.02 M H_3BO_3+0.1 M Na_2SO_4+0.1 M K_2SO_4+0.02 M $Fe_2SO_4 \times 7H_2O$+ 0.01 M H_2SO_4 solution. In a first stage, a potentiostatic iron deposition process was followed by chronoamperometry applying −1.3 V and keeping the overall charge for deposition at 3 °C. After this procedure, the electrode was washed and immersed in a solution containing 0.02 M H_3BO_3+0.1 M Na_2SO_4+ 0.1 M K_2SO_4 + 0.02 M $K_4[Fe(CN)_6]\times 3H_2O$+0.01 M H_2SO_4 where an oxidation scan at 1 mV/s from −1.2 V to −0.4 V was done. Later, this substrate was transferred to a 0.5 M K_2SO_4 solution and the subsequent voltammogram was recording.

For the optical characterization, PB deposition was carried out by means of cyclic voltammetry in a 0.01 M $FeCl_3$+0.01 M $K_3[Fe(CN)_6]$+1 M KCl solution at pH=1 adjusted by HCl. The potential limits were between −0.7 V to 0.25 V at 50 mV/s under illumination during 10 cycles and 30 cycles at room temperature.

The voltammetric measurements were carried out under illumination unless the opposite is indicated. Illumination was performed with a xenon lamp of 75 W (Oriel Instruments 6263) mounted in a lamp holder (Oriel 66902) and using a water filter (Oriel 61945) and a 1 m length optical fibre (Oriel 77578). A power supply of 40–200 W (Oriel 68907) was used to generate the arc in the lamp. The illumination power was quantified inside the cell by means of a power metre (Oriel 70260). The samples illuminated with the Xe lamp reach a light intensity of 4.0 mW cm^{-2}. A pure argon stream was passed through the solution for 30 min before measurements, and over the solution during the experiments.

The electrochemical measurements (cyclic voltammetry) were performed using Princeton Applied Research model 273A equipment.

Structural characterization of PB was examined by X-ray diffraction (XRD) with a Philips PW3710 diffractometer using CuK_α radiation (i.e. X-ray radiation wavelength: $\lambda_X = 1.54A$). The accelerating voltage was set at 40 KV with a 25 mA flux. Scatter and diffraction slits of 1° and collection slit of 0.1 mm were used. The energy dispersive X-ray analysis (EDS) was done with the use of a THERMO NORAND VANTAGE (with a NORVARD window, and a NORAN System 7 SPECTRAL IMAGING SYSTEM from Thermo Fischer Scientific) equipment installed in the JEOL 5900 LV Scanning Electron Microscope. Optical reflectance spectra were measured by means of an S2000 Ocean Optics fibre optic spectrometer, with a 50-mm fibre (acting as input slit), a Sony ILX511 Linear CCD Array, and an ISP-REF illuminated integrating sphere. The effective optical range of this equipment is 350–1,000 nm. A WS-1 Ocean Optics white diffuse reflectance standard was used as reference. Both spectra including and excluding specular reflectance (as allowed by the integrating sphere) were taken. In each case the reference spectrum were taken under the same conditions.

Results and discussion

Photoelectrochemical characterization of p-Si/PB electrodic system

After precipitation process, the p-Si/PB interface was immersed in a 0.5 M K2SO4 solution where the corresponding voltammetric profiles were registered. The characterization was assisted by illumination because in darkness conditions no response of the system was observed. The results are shown in Fig. 1.

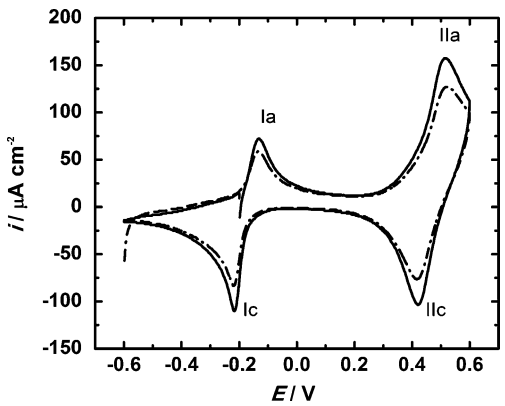

Fig. 1 Potentiodynamic i/E profiles of a p-Si/PB electrode under illumination in 0.5 M K_2SO_4 solution. *Solid line* 1st cycle; *dashed dotted* 2nd cycle

In Fig. 1, it is possible to observe two cycles corresponding to the characterization of p-Si/PB modified electrode. The potentiodynamic sweep was carried out from negative potential values (−0.6 V) toward positive potentials. In this profile appears redox processes associated to the high-spin iron, I_a (−0.13 V) and I_c (−0.216 V). For the response I_a, let us consider a hole (h^+) transfer from the valence band of silicon to the donor redox state in the PB film:

$$K_2\left\{Fe^{II}_{HS}\left[Fe^{II}_{LS}(CN)_6\right]\right\}_{(s)} + h^+_{BV} \rightarrow K\left\{Fe^{III}_{HS}\left[Fe^{II}_{LS}(CN)_6\right]\right\}_{(s)} + K^+_{(aq)} \quad (1a)$$

The conjugated process, I_c, is associated with the transfer of photogenerated electrons from the conduction band of silicon to PB film according to:

$$K\left\{Fe^{III}_{HS}\left[Fe^{II}_{LS}(CN)_6\right]\right\}_{(s)} + K^+_{(aq)} + e^-_{CB} \rightarrow K_2\left\{Fe^{II}_{HS}\left[Fe^{II}_{LS}(CN)_6\right]\right\}_{(s)} \quad (1b)$$

Toward more positive potential values appear responses attributed to the low-spin iron centre II_a (0.513 V) and would correspond to:

$$K\left\{Fe^{III}_{HS}\left[Fe^{II}_{LS}(CN)_6\right]\right\}_{(s)} + h^+_{BV} \rightarrow \left\{Fe^{III}_{HS}\left[Fe^{III}_{LS}(CN)_6\right]\right\}_{(s)} + K^+_{(aq)} \quad (2a)$$

The same way, the conjugated processes, II_c:

$$\left\{Fe^{III}_{HS}\left[Fe^{III}_{LS}(CN)_6\right]\right\}_{(s)} + K^+_{(aq)} + e^-_{CB} \rightarrow K\left\{Fe^{III}_{HS}\left[Fe^{II}_{LS}(CN)_6\right]\right\}_{(s)} \quad (2b)$$

In all processes, an intercalation of potassium ions in the structure is produced to ensure the electroneutrality. The same response has been obtained for PB onto different substrates [8–15]. Considering the difference between the anodic and cathodic peak potentials for both redox processes, it is possible affirm that corresponding to quasi-reversible responses, with a difference between of them of 86 and 95 mV for the high and low-spin iron centre, respectively. This quasi-reversibility behaviour for the p-Si/PB interface, delivery encouraging results, indicating the possibility to be studied as a storaging charge system [16–18]. However, a charge analysis between QIA/QIC and QIIA/QIIC indicate a ratio of 1.9 and 2.2, respectively. These results indicate that an anodic process is coupled to the oxidation of iron centres present in PB. Also, this ratio is increased when the anodic potential increase which indicates that the electrochemical substrate oxidation add a component to the anodic response. In fact, the oxide formation can be responsible of decrease of signals in the second cycle.

XRD analysis of p-Si/PB

Figure 2a shows the XRD data for a PB sample grown onto a p-Si(100) substrate from cyclic voltammetry (30 cycles),

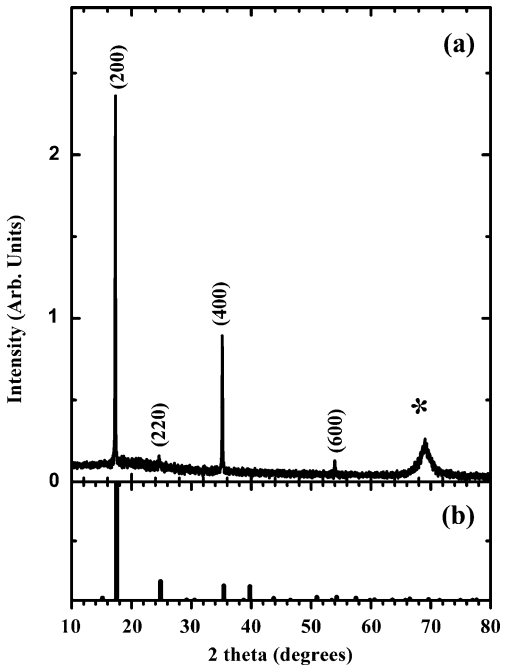

Fig. 2 XRD data for samples p-Si/PB (**a**) and JCPDS standard [19] (**b**)

while Fig. 2b shows the relative intensity according to JCPDS standard for $Fe_4(Fe(CN)_6)_3$ [19], which corresponds to a face centred cubic structure [20, 21]. Two larger peaks are clearly identified at 17.3° and 35.2°, while two smaller ones can also be assigned at 24.6° and 54.0°. No more peaks are present, except for the one close to 69° (marked with an asterisk in the figure), which can be assigned to silicon substrate (400) direction [22], in agreement with substrate orientation. The former ones are labelled as (200), (400), (220) and (600), in accordance with JCPDS standard that assign them to the following positions: 17.495°, 35.415°, 24.839°, and 54.289°, respectively [19]. The presence of the three major peaks corresponding to planes parallel to the (100) one, implies that the PB film is highly oriented along the preferred orientation of the Si substrate. Meanwhile the (220) peak appears because its intensity is the second most important in the JCPDS pattern [19]. However, all peak positions are slightly shifted to smaller angles. As the PB film reproduces the preferred orientation of the substrate, this can be due to a lattice mismatch between both structures. The reported lattice constants for each structure are a_{PB}=10.13 nm for PB [19] and a_{Si}= 5.43 nm for Si [22]; i.e. $a_{PB} \lesssim 2a_{Si}$. Therefore PB film may be stressed due to lattice mismatch, with a higher lattice constant, generating the diffraction angle shifts. In effect from the data peak positions a lattice constant of 10.21± 0.03 nm is obtained. This small departure of lattice constant from JCPDS standard [22] is commonly reported both in bulk [23] and in nanostructures of this material [24, 25]. The typical nanocrystallite size D in these samples can be found from diffraction peaks broadening, β. Scherrer

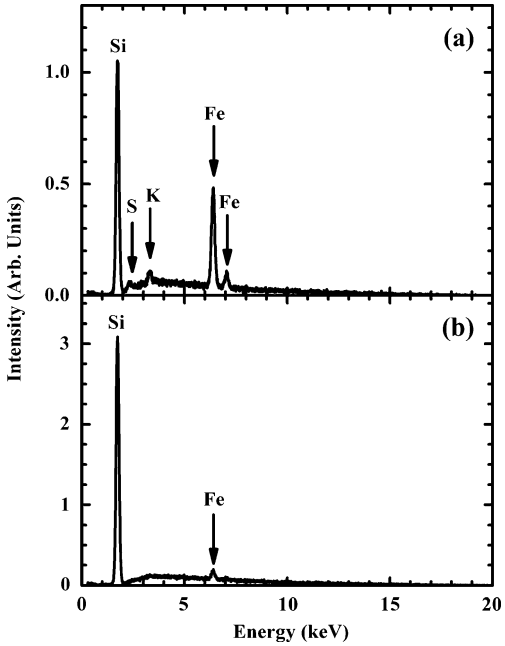

Fig. 3 EDS spectra for p-Si/PB samples synthesized from 30 voltammetric cycles (**a**) and ten cycles (**b**)

equation is the usual way of obtaining D [26–28]. However, in the present case a dependence of β with the diffraction angle θ is observed. Therefore, as all observed peaks are parallel to the (100) one, a Williamson–Hall approach was used to obtain simultaneously nanocrystallite size and microstrain [29]. In this approach, β must depend on θ according to:

$$\beta \cos\theta = \frac{K\lambda_X}{D} + 4\varepsilon \sin\theta \qquad (3)$$

where K is a constant close to 1 (K=0.9 was used for the present work), $\lambda_X = 1.54$A is the X-ray wavelength, β is the line broadening (full width at half maximum of the peaks in Fig. 2), while θ is the Bragg angle (half angle between incident and diffracted beams) at the centre of the peak. From a linear fitting of $\beta \cos\theta$ vs. $\sin\theta$ the values of D=120 nm and $\varepsilon = 6.4\times10^{-4}$ were found. This nanocrystallite size D is close to the limit of validity of this method [30], so no nanocrystalline effects are expected in the present case.

Moreover, other metal hexacyanoferrates have similar structure as the one observed in Fig. 2 (for example $Cu_2(Fe(CN)_6)$ [31]). Thus, to confirm that $Fe_4(Fe(CN)_6)_3$ is present in different samples, an EDS analysis were carried out for two samples of p-Si/PB formed by means of cyclic voltammetry and at different cycle numbers. Figure 3 shows typical results. Although the equipment does not detect lighter elements (like C and N) this figure shows major peaks corresponding to Fe and Si (coming from the substrate). No other metallic element appears but for some traces of K and S in Fig. 4a (2.1% and 2.6% atomic percentage, respectively). These signals can be associated to the potassium present in the PB structure and sulphur coming from the sulphate solutions. Furthermore, the relation of Fe to Si peak intensities is higher in Fig. 3a than in Fig. 3b. This may indicate that the corresponding PB film deposited from ten cycles (Fig. 3b) is thinner than the one deposited from 30 cycles with the voltammetric method.

Additionally, and considering the bluish coloration to the naked eye for all synthesized samples, optical reflectance was measured. Figure 4 shows the results of these

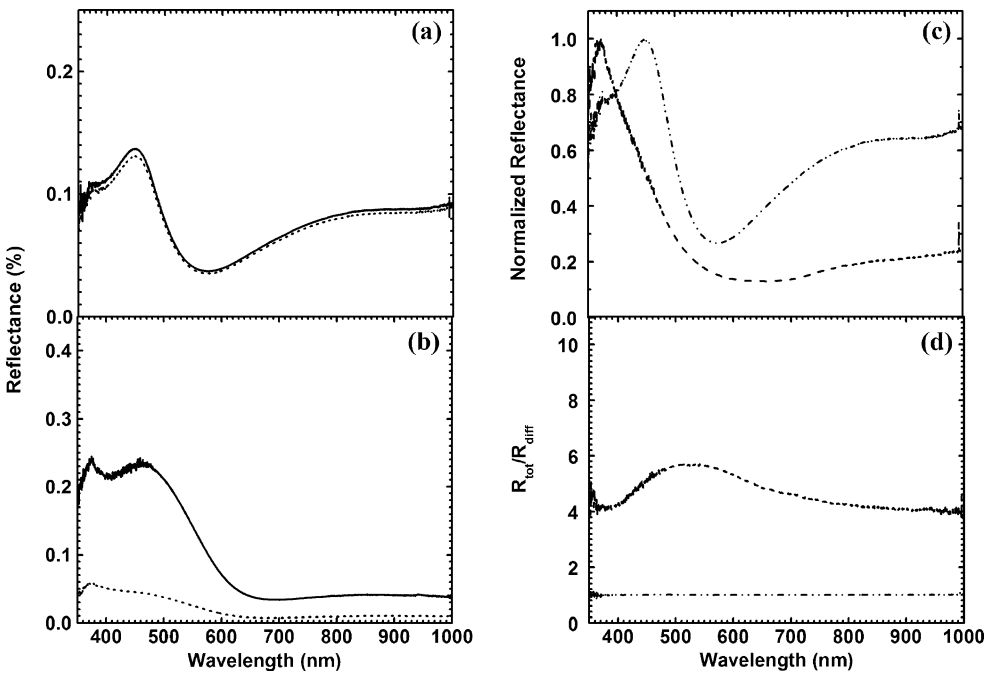

Fig. 4 Optical reflectance spectra for samples synthesized from cyclic voltammetry 30 cycles (**a**); ten cycles (**b**). In these figures, *solid line* includes specular reflectance while *short dashed line* excludes it. In (**c**), the normalized spectra are compared, while in (**d**) the ratio between the reflectance spectra for each sample are shown. In (**c** and **d**), *dashed* and *dashed double dotted* lines are for p-Si/PB samples synthesized from ten to 30 voltammetric cycles, respectively

Table 1 Resumé of optical properties: tristimulus values (*X*, *Y*, and *Z*) and chromatic coordinates (*x* and *y*), according to CIE 1931 standard and peak wavelength (λ_{peak}) of KM function obtained from Fig. 5

Sample	Spectra	*X*	*Y*	*Z*	*x*	*y*	λ_{peak} (nm)
10 cycles (Fig. 4a)	R_{diff}	2.03	2.32	4.43	0.232	0.264	686
	R_{tot}	10.7	12.9	22.7	0.232	0.278	–
30 cycles (Fig. 4b)	R_{diff}	5.39	4.61	11.9	0.247	0.211	575
	R_{tot}	5.65	4.84	12.4	0.247	0.211	–

measurements for both samples presented in Fig. 3, where Figs. 4a, b correspond to the p-Si/PB samples synthesized from 30 and ten voltammetric cycles, respectively. Additionally, Figs. 4a, b show the spectra with short dashed lines the diffuse reflectance R_{diff} (i.e. excluding specular reflectance), while those shown with full lines represent the total reflectance R_{tot} (i.e. including specular reflectance), respectively. Figure 4c compares the (normalized) diffuse reflectance spectra for the two different cases, while Fig. 4d shows the ratio between the total and diffuse spectra. For both samples either reflectance spectra R_{diff} and R_{tot} have maximum values in the blue–UV region, which corresponds to their colour. Table 1 shows, for each spectra in Figs. 4a, b, the chromatic coordinates calculated according to CIE 1931 standard [32, 33] under pure white (flat spectrum) illumination. These coordinates correspond to points among the blue, greenish blue and purple region of the chromaticity diagram. It is seen that for the sample synthesized from 30 voltammetric cycles the values do not change for spectra including or excluding specular light. This is because the spectra of R_{diff} and R_{tot} are very similar. For the sample obtained from ten voltametric cycles, there is some difference in the results for each spectrum. This is because the sample is glossier than the others. A measurement of the glossiness of a sample is given by the relation between the total and diffuse reflectance. This ratio R_{tot}/R_{diff} varies between 4.0 and 5.7 (with maximum at 520 nm) for this sample. For the sample p-Si/PB from 30 cycles, this ratio is almost flat and equal to 1 in all the spectra revealing their perfect matte appearance.

The PB optical properties are governed by absorption bands [30, 34] that are usually assigned to charge transfer processes [28, 35]. Calculations of electronic band structure based on general consensus of PB being an intrinsic semiconductor predicts an absorption edge at 1.21 eV (~1,025 nm), approximating the 1.75 eV value corresponding to the observed 700 nm band [23]. This model allows understanding the optical absorption as the excitation of a charge transfer process from *d*-orbitals from Fe(II) to *d*-orbitals in Fe(III), both from electronic states intensities and density of states [23]. As a way to understand if this is the origin of the structures observed in the optical reflectance spectra of Fig. 4, the Kubelka–Munk (KM) function $F_{KM}(R)$ was calculated form diffuse reflectance spectra [33, 36]. This function is defined as:

$$F_{KM}(R) = \frac{(1-R)^2}{2R} \tag{4}$$

being $R=R_{diff}$. In Kubelka–Munk phenomenological theory, for samples infinitely which are thick, this function is equal to the ratio between the absorption coefficient *K* and the scattering coefficient *S*. In samples where a small fraction of a powder of the material under study is mixed with a white non-absorbing powder, *K* is small and *S* can be assumed to be independent of wavelength, so the KM function is a direct measurement of absorption coefficient. In other cases, corrections to this approximation are needed [37, 38]. As in the present case, the samples under study are compact films, the approximations are not valid, and so the KM function is just calculated as a quantitative comparison between samples. In spite of that, the resulting spectrum, which is shown in Fig. 5, corresponds with absorption bands in the region between 550 to 750 nm [30, 39]. The overall spectral KM function for the sample synthesized from 30 voltammetric cycles the peak position is blue shifted against those

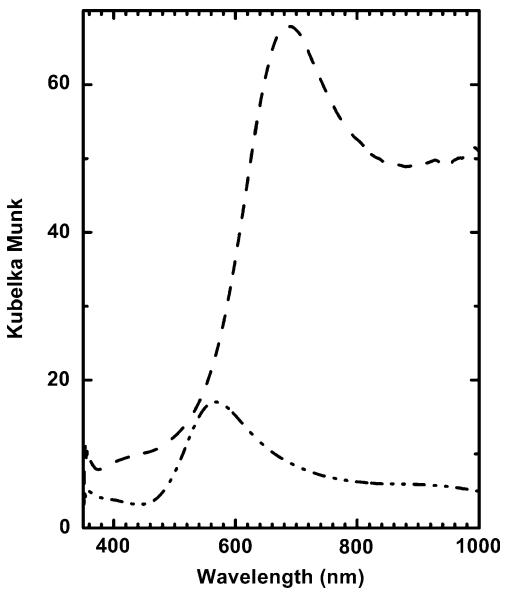

Fig. 5 Kubelka–Munk function for p-Si/PB samples synthesized from ten (*dashed line*) to 30 voltammetric cycles (*dashed double dotted line*)

sample formed from 10 cycles, although the spectra corresponding to this one extend into the IR region. The different colours observed in Table 1 may be attributed to the shifts in these peak positions, which are also shown in the last column of this table. Similar shifts observed in the literature were assigned to nanometric effects [28, 35]. However, in the present case, no nanometric effects were found in XRD (Fig. 2), although the EDS spectra show a small content of K element (Fig. 4a). Therefore the question is how this K content may influence the optical properties. Recently it was shown by first principle calculations of electronic structure that changes in stoichiometry lead to two different forms of PB called "soluble" (with K) and "insoluble" (without K) [40]. The "soluble" form has an energy bandgap of 1.7 eV (~730 nm), that is blue shifted to 1.9 eV (~653 nm) for the "insoluble" form. This shift is in the opposite direction compared with the one observed here, but previous calculations also shown the appearance of new bands in the infrared region. Nothing that KM function for the sample from ten cycles has a relative important value into the IR region, and information their spectra are wider than for the sample synthesized from 30 cycles.

Conclusions

The study about PB characterization on p-Si(100) by means of cyclic voltammetry under illuminations conditions indicated the presence of redox processes assigned to high and low-spin iron centres which present a quasi-reversibility behaviour. However, an anodic parallel reaction appears in the voltamogram which was attributed to the silicon oxide formation which is the responsible for the difference between the anodic and cathodic charge. Considering the XRD measurements, crystalline PB was formed. The planes observed in the difractogram indicate a parallel growth of PB to the silicon substrate. Also, no nanocrystallite size effect was founded through Williamson–Hall approach. The EDS results indicated the presence of Fe. K was attributed at its presence in the PB structure and S due to the sulphate solutions employed. An increase in the cycles for the PB formation, produced an increase in the Fe signals which is an indicative of thicker deposits. Reflectance measurements showed maximum values in the blue–UV region. Considering chromatic coordinates from CIE 1931 standard the samples showed points among blue, greenish blue indicating a mix between hexacyanometallates deposited onto silicon: for instance Prussian blue and Berlin green.

Acknowledgements We thank FONDECYT, Chile, for financially supporting this study (grant N° 1090217) and the Dirección de Investigación e Innovación of the Pontificia Universidad Católica de Valparaíso (grant no. 037.108/2008 DII-PUCV). E. Muñoz and R. Henríquez thank the Programa Bicentenario de Ciencia y Tecnología, PSD82. R. E. Marotti and Enrique A. Dalchiele also acknowledge the support received from CNPq (Brazil, Prosul Program, Project # 490580/2008-4), PEDECIBA-Física, ANII (Administración Nacional de Investigación e Innovación) and the CSIC (Comisión Sectorial de Investigación Científica) of the Universidad de la República, in Montevideo, Uruguay. Special thanks to Fritz Scholz of the Ernst-Moritz-Arndt-Universität Greifswald for his collaboration on the discussion of this work.

References

1. Muñoz EC, Schrebler RS, Orellana M, Córdova R (2007) J Electroanal Chem 611:35–42
2. Muñoz EC, Schrebler RS, Grez P, Henríquez R, Heyser C, Verdugo P, Marotti R (2009) J Electroanal Chem 633:113–120
3. Muñoz EC, Henríquez R, Schrebler RS, Heyser C, Verdugo P, Marotti R (2009) Thin Solid Films 518:138–146
4. Schrebler R, Muñoz E, Cury P, Suárez C, Gómez H, Córdova R, Dalchiele E, Marotti R (2006) J Phys Chem B 110:21109–21117
5. Muñoz EC, Schrebler RS, Córdova R, Marotti R, Dalchiele E (2007) J Phys Chem B 111:16505–16515
6. Oskam G, Vereecken PM, Searson PC (1999) J Electrochem Soc 146:1436–1441
7. Istratov AA, Weber ER (2002) J Electrochem Soc 149:G21–G30
8. Orellana M, Ballesteros L, Del Río R, Grez P, Schrebler R, Córdova R (2009) J Solid State Electrochem 13:1303–1308
9. Zamponi S, Kijak AM, Sommer AJ, Marassi R, Kulesza PJ, Cox JA (2002) J Solid State Electrochem 6:528–533
10. Agrisuelas J, Gabrielli C, García-Jareño JJ, Giménez-Romero D, Gregori J, Perrot H, Vicente F (2007) J Electrochem Soc 154: F134–F140
11. Pyrasch M, Toutianoush A, Jin W, Schnepf J, Tieke B (2003) Chem Mater 15:245–254
12. Zhao H, Yuan Y, Adeloju S, Wallace GG (2002) Anal Chim Acta 472:113–121
13. Ellis D, Eckhoff M, Neff VD (1981) J Phys Chem 85:1225–1231
14. Viehbeck A, DeBerry DW (1995) J Electrochem Soc 132:1369–1375
15. Orellana M, Arriola P, Del Río R, Schrebler R, Cordova R, Scholz F, Kahlert H (2005) J Phys Chem B 109:15483–15488
16. Eftekhari A (2003) J Power Sources 117:249–254
17. Jayalakshmi M, Scholz F (2000) J Power Sources 87:212–217
18. Eftekhari A (2003) J Mater Sci Lett 22:1251–1253
19. JCPDS File No. 73-0687 (1999) (Iron cyanide)
20. Hermes M, Scholz F (1997) J Solid State Electrochem 1:215–220
21. Herren F, Fischer P, Ludi A, Hãlg W (1980) Inorg Chem 19:956–959
22. JCPDS File No. 05-0565 (1999) (Silicon)
23. Wojdel JC, Bromley ST (2004) Chem Phys Lett 397:154–159
24. Shan Y, Yang G, Gong J, Zhang X, Zhu L, Qu L (2008) Electrochim Acta 53:7751–7755
25. Pan Q, Huang K, Ni S, Yang F (2009) Mater Res Bull 44:388–396
26. Cullity BD (1978) Elements of X-ray Diffraction. Addison-Wesley, Masachussetts
27. Klug HP, Alexander LE (1954) X-ray diffraction procedures for polycrystalline and amorphous materials. Wiley, New York
28. Vo V, Minh NV, Lee HI, Kim JM, Kim Y, Kim SJ (2009) Mater Res Bull 44:78–81
29. Enríquez JP, Mathew X (2003) Sol Energy Mater Sol Cells 76:313–322
30. Agnihotry SA, Singh P, Joshi AG, Singh DP, Sood KN, Shivaprasad SM (2006) Electrochim Acta 51:4291–4301

31. JCPDS File No. 86-0514 (1999) (Copper iron cyanide)
32. Brainard DH, Colorimetry (1996) In: Bass M, Van Stryland EW, Williams DR, Wolfe WL (eds) Handbook of Optics. McGraw-Hill, New York
33. Torrent J, Barrón V (2002) Diffuse reflectance spectroscopy of iron oxides. In: Hubbard AT (ed) Encyclopedia of Surface and Colloid Science, 2nd edn. CRC Press, New York
34. Zhang D, Wang K, Sun D, Xia X, Chen H (2003) J Solid State Electrochem 7:561–566
35. Vo V, Van MN, Lee HI, Kim JM, Kim Y, Kim SJ (2008) Mater Chem Phys 107:6–15
36. Schröder U, Scholz F (1997) J Solid State Electrochem 1:62–67
37. Loyalka SK, Riggs CA (1995) Appl Spectrosc 49:1107–1110
38. Boroumand F, Moser JE, den Bergh H (1992) Appl Spectroscopy 46:1874–1879
39. Zakharchuk NF, Naumov N, Stösser R, Schröder U, Scholz F, Mehner H (1999) J Solid State Electrochem 3:264–276
40. Wojdel JC (2009) J Mol Model 15:567–579